# Rewritable, Moldable, and Flexible Sticker-Type Organic Memory on Arbitrary Substrates

*Ying-Chih Lai, Yi-Xiang Wang, Yi-Chuan Huang, Tai-Yuan Lin, Ya-Ping Hsieh, Ying-Jay Yang, and Yang-Fang Chen**

**Fabrication of functional devices on arbitrary non-conventional substrates has significant advantages for broadening devices applications and the development of soft electronic systems such as flexible, stretchable, wearable, and epidermal electronic modules. Information storage device is one of crucial electronic elements in modern digital circuitries. Herein, a re-writable, transferable, and flexible sticker-type organic memory on universal substrates is demonstrated through a facile and cost-effective one-step strategy. The organic memory sticker based on the graphene electrode grown by chemical vapor deposition consists of a blending composite of polymer (poly (methyl methacrylate) (PMMA):poly (3-hexylthiophene) (P3HT) in chlorobenzene (CB) fabricated by mature solution processes and facilities. By combining with the mechanical elastic of organic material and graphene electrode, the sticker-type organic memory can be easily tagged on non-planar or flexible substrates after etching away the supporting metal. Particularly, the new attachable sticker-type memory processes a unique feature of re-programmable capability. It is believed that the universal substrate selectivity of the sticker-type organic memory with re-writable characteristic revealed here may greatly enlarge information storage devices in immense areas and advance the future functional soft circuitries.**

Y.-C. Lai, Prof. Y.-F. Chen
Department of Physics
National Taiwan University
No. 1, Sec. 4, Roosevelt Road, Taipei, 106, Taiwan, Republic of China
E-mail: yfchen@phys.ntu.edu.tw
Y.-C. Lai, Prof. Y.-J. Yang
Graduate Institute of Electronics Engineering
National Taiwan University
No. 1, Sec. 4, Roosevelt Road, Taipei, 106, Taiwan, Republic of China
Y.-X. Wang
Graduate Institute of Applied Physics
National Taiwan University
No. 1, Sec. 4, Roosevelt Road, Taipei, 106, Taiwan, Republic of China
Y.-C. Huang, Prof. T.-Y. Lin
Institute of Optoelectronic Sciences
National Taiwan Ocean University
No.2, Pei-Ning Road, Keelung, 224, Taiwan, Republic of China
Prof. Y.-P. Hsieh
Graduate Institute of Opto-Mechatronics
National Chung-Cheng University
No. 168, Sec. 1, Daxue Rd., Minxiong Township, Chiayi County, 621, Taiwan, Republic of China
Prof. Y.-F. Chen
Center for Emerging Material and Advanced Devices
National Taiwan University
No. 1, Sec. 4, Roosevelt Road, Taipei, 106, Taiwan, Republic of China

**DOI: 10.1002/adfm.201302246**

## 1. Introduction

Flexibility, stretchability, portability, and transparency are anticipated specifications in future electronic applications such as paper-like display, wearable computer, and epidermal electronics.[1] A crucial challenge for those future electronic circuitries is how to fabricate and integrate multiple flexible and stretchable electronic devices onto a polymeric or nonconventional substrate. This hurdle arises from the fact that those nonconventional substrates are suffered from difficult handling requirements and poor tolerance for high temperature and chemical processing. An important research progress for those future electronic modules is urged to develop suitable manufacturing strategies for fabricating functional electronics on desired arbitrary substrates.[2–8] Successful progress has been reported on different devices such as transferable transistors,[4] light-emitting diodes (LEDs),[6] sensors,[9] and power supplies.[7]

Information storage device, which has been omnipresent in the modern digital age, is one of the critical and fundamental components in all commercial electronic systems.[10] Recent progress in resistive switching memories,[11,12] based on switching behavior of electrical conductivity, has effectively simplified the complicated traditional flash memory by using a simple sandwich configuration, promising the possible integration of information storage devices into those advanced electronic systems such as flexible display and wearable electronics.[13] Among various materials, organic bistable resistive memories have attracted much attention due to their exceptional advantages of low-cost, low-temperature process, 3D-stacked capacity, and solution-printability.[14–16] In particular, the unique properties of elasticity and flexibility of organic materials promise their great potential in future foldable and stretchable electronic systems.[17,18] However, the solution processes of organic materials block them from vertical integration with other organic devices, such as organic transistors, diode and power supply, because they will confront fatal dissolving problems to the bottom organic devices and even the soft polymeric substrates.[19,20] It therefore obstructs the digital organic storage devices to function in those future advanced

soft electronics. So far, these information storage devices have been fabricated only on conventional substrates, such as rigid, flat, and smooth surface, which further limits their promisingly immense applications on universal substrates.[16] Thus, in order to broaden the information storage device applications and pave a way to integrate digital memory devices in future soft electronic modules, it is greatly important to develop an efficient scheme for fabricating organic memories onto desired substrates.

Graphene, the thinnest two dimensional carbon crystal, is a remarkable material due to its superior physical and electrical properties.[21] Owing to the excellent electron-transfer characteristics, mechanical flexibility and stretchability, together with its optical transparency and low-cost features, graphene sheets have been considered as the next-generation conductor for flexible and wearable electronics.[22–28] Successful growth graphene film by chemical vapor deposition (CVD) method enables efficiently to place a large-area graphene film onto arbitrary substrates, after post-etching the supporting metal, by suitable transferring methods.[23,29,30] Notably, its astonishing mechanical properties, such as intrinsic strength of 42 N $m^{-1}$ and Young's modulus of ≈1 TPa, addition with strong attractive interfacial adhesion force, that is, Van der Waals (adhesive energy of 0.45 J $m^{-2}$ on $SiO_2$) make the CVD-growth graphene as a great interfacial electrode for attaching onto nonconventional surface and flexible electronic applications.[31] Moreover, graphene exhibits a good interfacial contact and lower contact resistance with organic materials.[32] Therefore, combining with the above merits, the integration of organic materials and the flexible graphene electrode opens a promising scheme for molding the organic memory onto a desired non-conventional surface, and meanwhile, it possesses a ready-to-conduct graphene underlay with self-adhesive feature, that is, called a sticker-type organic memory.

In previous reports, Liu et al. have demonstrated excellent write-once-read-many (WORM)-type and re-writable memories by using reduced graphene oxide (rGO) film,[33,34] and Ji et al. have realized a flexible WORM-type memory by using multilayer graphene as flexible top electrodes.[17] However, the tortuous reduction and laminated process for the flexible graphene electrodes might sacrifice the easy fabrication merits of organic memories. Also, the bottom-up spin-coating processes for the organic active layer limits the resulting memory devices on conventional substrates. Previously, we have reported a transferable and flexible WORM-type memory based on CVD-graphene by a facile integrated strategy.[35] The resulting organic WORM-type memory can be simply transferred onto arbitrary substrates, including soft, rough, non-planar ones, or even an organic device. However, the one-time only programmable and un-rewritable feature of the WORM-type memory is a great drawback for mass-practical applications.

Herein, we report a new transferable and flexible sticker-type organic resistive memory with erasable capability, which represents the first example of a re-writable sticker-type organic memory (RSOM). Our result demonstrates that the RSOM can be simply stuck on various desired substrates, including rigid, flexible, non-planar, and rough substrates, and so forth, promising that the information storage devices can be greatly broadened in diversified future applications. The RSOM is based on a sandwich structure of CVD-growth graphene/poly(methyl methacrylate) (PMMA): poly(3-hexylthiophene) (P3HT)/Al. The polymer composite of mixed PMMA and P3HT in chlorobenzene (CB) can be simply spin-coated onto the prepared CVD-growth graphene on the supporting copper foil. In addition to acting as the memory active layer, the polymer composite can also serve as the protective layer during the CVD-graphene stripping process. Thus, the fabrication processes can be significantly reduced, rendering our strategy to be quite beneficial for low-cost and large-scale fabrication of organic memories. Especially, saving in the chemical treatment for washing away the protective layer from CVD-graphene enables the memory application on arbitrary non-conventional and polymeric substrates and vertical integration with other organic devices. Also, the presented work is based on low-temperature, well mature fabrication processes and facilities, promising the sticker-type memory practically feasible for future soft electronics. According to the capability of roll-to-roll fabrication process for CVD-graphene,[36] the presented retrievable sticker-type memory might be industrial-friendly for mass production.

## 2. Results

### 2.1. Device Structure

**Figure 1**a illustrates the schematic fabrication processes for the RSOM. The large area of graphene film was synthesized on copper foil using typical CVD technique.[37] The single-layer CVD-graphene with few defects was characterized by Raman spectroscopy (Figure S1 in Supporting Information) and the

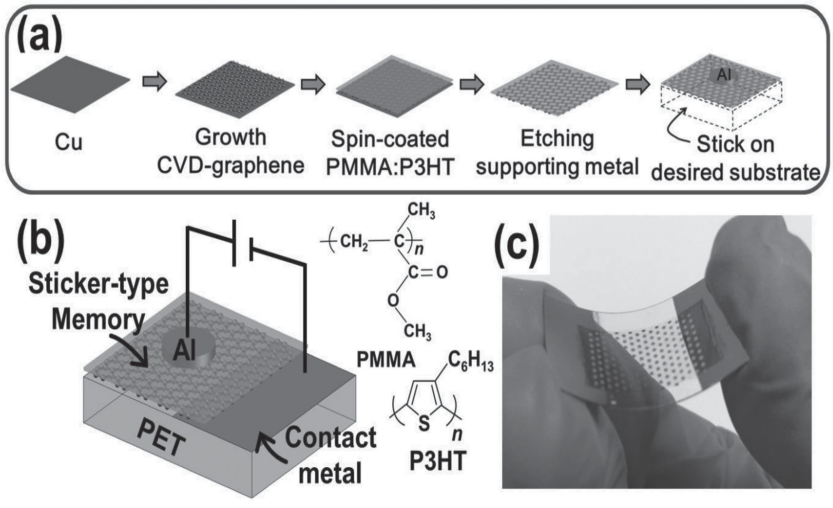


**Figure 1.** a) Schematic of the fabrication processes for the sticker-type organic memory. b) Arrangement for electrical measurement of RSOM along with the chemical structures of PMMA and P3HT. c) Photo of as-prepared RSOM under bending.

sheet resistance of the graphene sheet measured by four-point probe method is about ≈1.1 kΩ $sq^{-1}$. The as-prepared blending mixture composed of PMMA and P3HT in CB can be simply spin-coated on the graphene film and serves as the protective layer while stripping the graphene film as well as an active layer for the organic memory. After selectively etching away the supporting copper foil, the RSOM can be easily transferred on desired substrates. We first tagged the RSOM onto a flexible polyethylene terephthalate (PET) substrate for measuring its electrical switching behaviors. In order to probe the bottom graphene electrode, a contact metal (Ni) for the graphene was pre-deposited on the margin of the PET substrate and partially connected with the bottom graphene electrode. Figure 1b depicts the schematic of the measuring arrangement together with the chemical structures of PMMA and P3HT. Figure 1c shows the optical image of the finished RSOM labeled onto a PET substrate with highly bendable characteristics. Comparing the atomic force microscopy (AFM) image of PMMA:P3HT/graphene film before and after transferring processes (Figure S2 in Supporting Information), the transferred PMMA:P3HT/graphene film only shows a slightly wrinkled surface with no significant damage during the etching and transferring process.

### 2.2. Memory Device Measurements

The electrical switching behavior and bistable memory effect of the sticker-type memory (graphene/PMMA:P3HT/Al) are illustrated by the current–voltage (*I–V*) characteristics, as shown in **Figure 2**a. In the beginning, we measured the sticker-type organic memory on the PET under flat condition. The bias

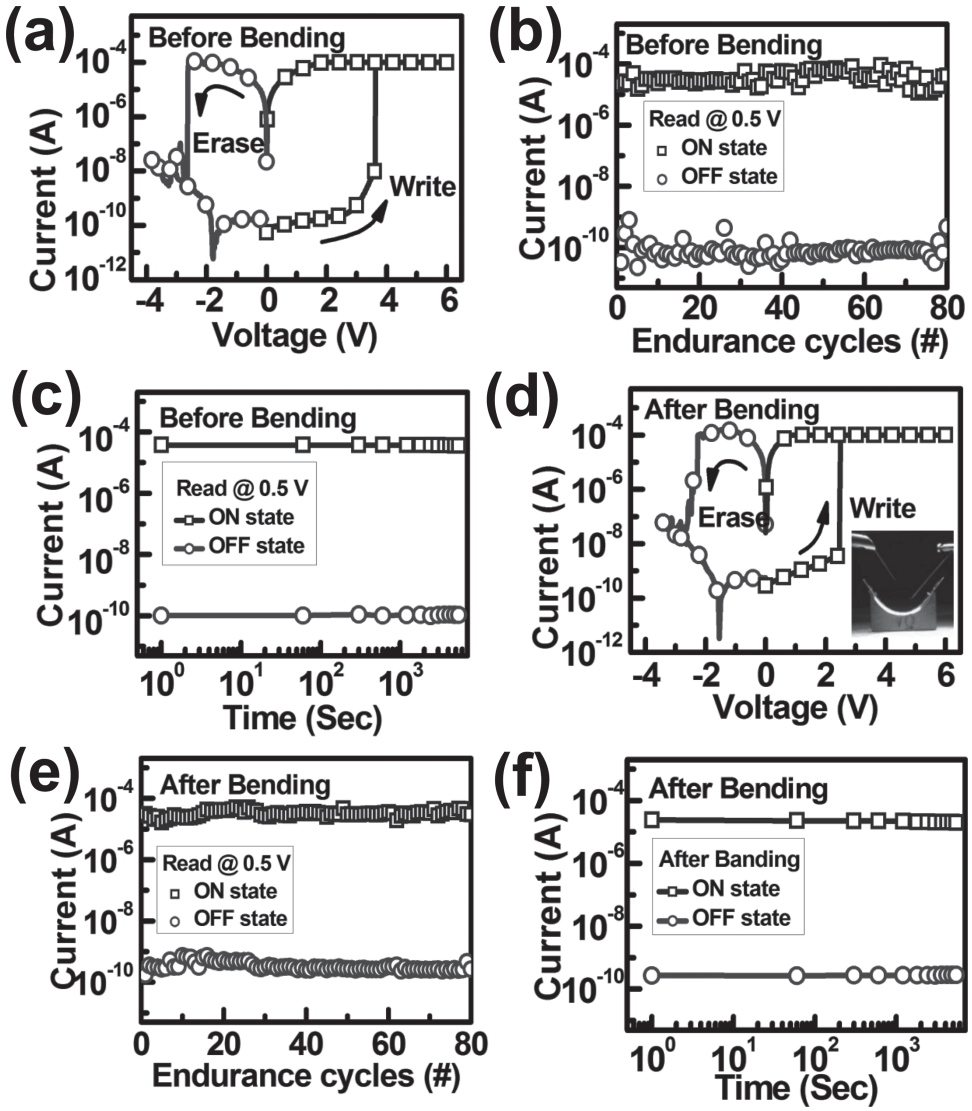


**Figure 2.** Electrical properties of the RSOM: a,d) *I–V* characteristics for the memory device on flat and bending conditions (bending radius R = 10 mm), respectively. The inset in (d) presents the image of the RSOM bent at *R* = 10 mm. b,e) The DC cyclic switching tests for the RSOM at the reading voltage of +0.5 V on flat and curvy conditions, respectively. c,f) The programmed data retention ability at the reading voltage of +0.5 V on flat and curvy conditions, respectively.

was applied onto the top Al electrode with an appropriate current compliance of 0.0001 A to prevent the device from hard breakdown, and the graphene electrode was grounded. The arrows point out the sweeping direction of the applied voltage. Initially, as the bias sweeping from 0 to 6 V, the current starts in a low-conductivity (OFF) state within a quit low current level of $\approx 10^{-10}$ A and increases monotonically in the low bias regime. As the applied bias is greater than the turn-on voltage (about +3.6 V), a sudden increase in the current flow from the low- (OFF) to the high-conductivity (ON) state is observed. This electrical switching behavior corresponds to the "writing" process in the digital storage device.[33] The programmed high-current state can be maintained during the sequential forward sweeping, indicating the nonvolatile feature of the memory. Typical values of the ON- and OFF-state currents at the reading voltage of 0.5 V are $10^{-5}$ A and $10^{-10}$ A, respectively, with a high ON/OFF ratio of $\approx 10^5$, making a ready recognition for the digital information ("0" or "1") programmed in the sticker-type memory. Afterward, as the bias is negatively swept with no current compliance, the programmed high-current state can be retrieved to the original low-conductivity (OFF) state at a suitable negative bias (about –2.6 V), indicating a rewritable feature of the memory effect. This reinstated process is equivalent to the "erasing" process in the digital memory applications.[38] The erased OFF state can be reprogrammed to the ON state again in the subsequent writing bias sweep. Thus, the *I*–*V* characteristic of the sticker-type memory exhibits a typical rewritable switching memory behavior.

In order to investigate the re-writability of the erasable sticker-type memory, such writing and erasing processes were cyclically switched by dc sweeping mode, and the current was read out at the reading voltage of 0.5 V in each cyclic sweep. As shown in Figure 2b, the device can be operated successfully more than 80 times, and still exhibits a large ON/OFF current ratio of about $10^5$. In addition, to assess the data retention ability of the memory, the OFF and programmed ON states were read out at the 0.5 V after regular intervals, respectively. Figure 2c shows the results that the OFF-state and coded ON-state currents were retainable in the programmed state with the same order for over 1.5 h. According to the above results, the sticker-type memory exhibits a reversible and steady bistable electrical memory behavior, promoting them widely used in commercial electronic systems, such as portable disks, smart pads, digital players and cameras, for nonvolatile information storage.

### 2.3. Information Storage Functions on Curvy Condition

For further evaluating the feasibility of the RSOM for flexible memory applications, the bistable switching behavior of the RSOM was examined after bending. As shown in the insert of Figure 2d, the memory sticker on PET was bent into a concave with surface curvature radius of 10 mm. The measurement condition was identical to the flat one. As represented in Figure 2d, the bended RSOM exhibits the resembling electrical hysteresis behaviors, indicative of its capability for digital information storage under different geometric conditions. The ON/OFF current ratio at the reading bias of 0.5 V under bending is about $10^5$ which is as large as its flat status, meaning that the manifest memory window is not swayed by the curvy situation. The associated cycling tests and retention ability were also employed to confirm its re-writability and memory performance after rolling deformation. Figure 2e shows that its re-writable capability and ON/OFF switching behaviors can work well even after 80 times of dc sweeping, indicative of the reproducibility for flexible memory applications. Moreover, the ON/OFF current ratio can be manifestly recognized more than 1.5 h, indicative of its retention ability is not affected after bending. Accordingly, the RSOM can maintain the excellent digital storage functions irrespective of its physical bending conditions, promising its application potential for data storage in flexible electronics and various surfaces.

### 2.4. Information Storage Functions on Arbitrary Substrates

Subsequently, in order to broaden the technical application of the electrically erasable sticker-type memory, we tried to transfer it onto various nonconventional substrates and test its electrical switching behaviors. The corresponding electrical measurements are presented alongside the photos of the RSOM on diverse substrates. Firstly, as shown in **Figure 3**a, the sticker-type memory can be easily transferred on a business card and manipulated unerringly. We have also tried to label the sticker-type memories onto various non-planar surfaces such as fake nail (Figure 3b) and rigid cylindrical vial (with a diameter of 20 mm) (Figure 3c) and measured their memory behaviors. The results show that the sticker-type memory can function normally regardless of its physical presentation. Figure 3d demonstrates the memory sticker operated on a bent medical wristband, illustrating its promising application in future flexible electronics for information storage. Next, the sticker-type memories were successfully placed onto a peelable 3M Post-it Tabs and 3M Scotch magic tape as depicted in Figures 3e,f, respectively, and both of the stuck memories exhibit regular bistable memory features. The peelable tapes enable the re-writable organic memory sticker removal and re-use on different substrates. As a result, the proposed RSOM based on the mechanically flexible and elastic graphene electrode and organic material can greatly expand the digital information storage applications on desired non-conventional substrates. Moreover, the fabricating processes shown here are very simple, low-temperature, and the sticker feature of the re-writable organic memory with no chemically washing away for the protective layer from graphene electrode may be also beneficial for the development of relevant areas, such as bendable, wearable and epidermal electronics. In addition, based on the roll-to-roll fabrication capability for CVD-graphene,[36] the presented memory sticker might be industry-friendly for large-scale manufacture.

## 3. Discussion

### 3.1. Discussion of the Electrical Switching Behaviors

In order to further understand about the charge transport of the RSOM and the underlying mechanism for the electrical conductivity transition, the measured *I*–*V* characteristics

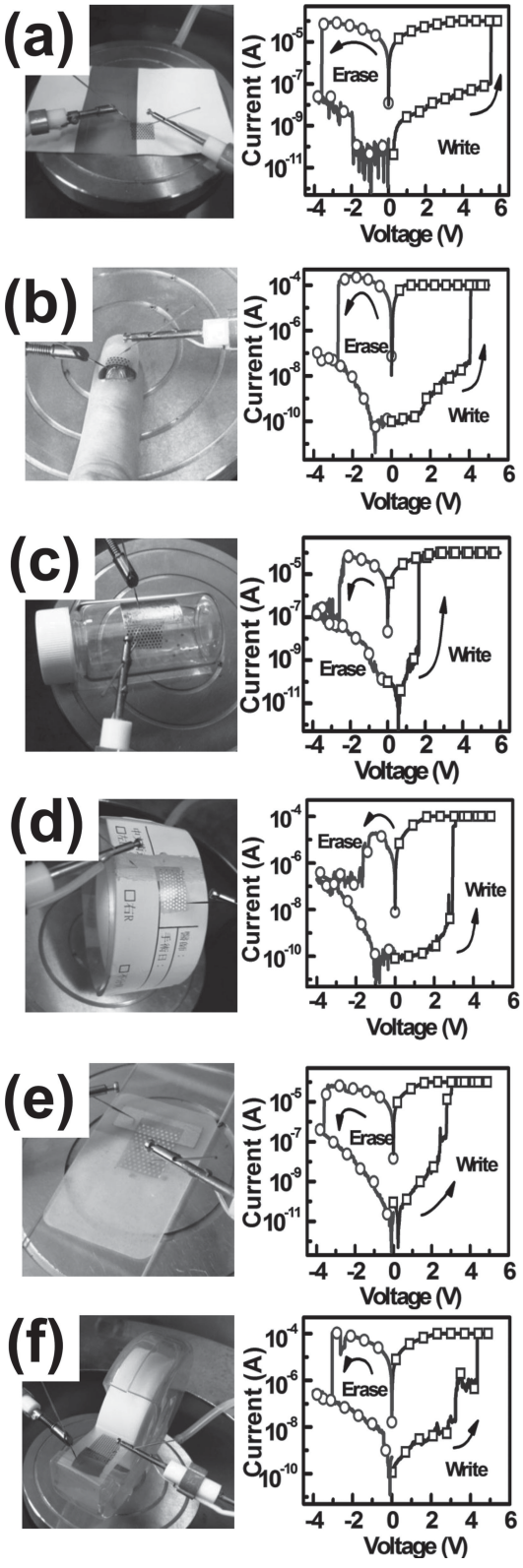


**Figure 3.** a–f) Demonstrations of the RSOMs labelled onto various non-conventional substrates with the corresponding *I–V* curves alongside, including on a) a business card, b) a fake nail, c) the outside surface of a cylindrical vial, d) a medical wristband, e) a peelable Post-it Flag, f) a 3M Scotch magic tape. (The area of RSOM is about 1 $cm^2$.)

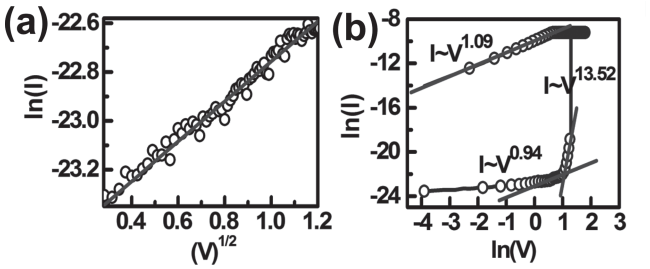


**Figure 4.** Experimental data and theoretical results of log–log plot of *I–V* measurements for RSOM. a) The OFF-state current below 1.5 V can be fitted by the Schottky emission model. b) The OFF-state current from 1.5 V to 3.56 V and the ON-state current can be fitted by SCLC and Ohmic model, respectively.

were firstly analyzed by different carriers transport models:[39]

a. Schottky emission (SE) conduction model, that is, thermionic emission with

$$I \propto AT^2 \exp\left[\frac{\phi_B - q\sqrt{qV)4\pi sd}}{kT}\right], \quad (1)$$

b. Space-charge-limited current (SCLC) conduction model with

$$I \propto V^{\alpha}, \quad (2)$$

c. Ohmic current conduction model with

$$I \propto V \exp\left(-\frac{\Delta E_{ae}}{kT}\right), \quad (3)$$

where $A$, $T$, $k$, $\phi_B$, $q$, $\varepsilon$, $d$, and $\Delta E_{ae}$ are the Richardson constant, temperature, Boltzmann constant, Schottky energy barrier, electron charge, dielectric constant, the thickness of the film, and the activation energy, respectively. As shown in **Figure 4**a, the current in the OFF state can be divided into three distinct regions to clarify the current transport mechanism. For the initial OFF-state current from 0 V to 1.5 V, the quite low current characteristics can be described by the SE current, that is, thermionic emission (Figure 4a). For the OFF-state current at the low biases range from 1.5 V to 2.6 V, the slope of the fitting line is 0.94, indicating that the Ohmic current dominated the device conduction in this regime (Figure 4b). The above fitting results suggest that the low OFF-state current below ≈2.6 V may be attributed to the charge carriers injected from the electrode into the polymer composite film after overcoming the energy barriers in the metal/polymer hetero interface. Afterward, for the OFF-state current range from 2.8 V to 3.56 V, the fitted slope of the increasing current yields $\alpha = 13.52$, indicating that the carriers transport follows a typical SCLC with a trap mode, that is, trapped charged-limit current (TCLC) mechanism.[40,41] Son et al. suggested that the slope with $\alpha >> 2$ may be in association with the fact that the carrier trapping sites exponentially distribute over the insulating PMMA polymer matrix.[42–44] In the present RSOM, the conjugated P3HT polymers are presumably responsible for the capture media of the transporting carriers.[45] Therefore, as a result of increasing the applied bias, the injected carriers from the electrode are captured by

the P3HT molecules and act as space charges at the high bias in the OFF state. Similar charge trapping phenomena have been reported in the literatures regarding hybrid-type inorganic/organic polymer memories or small molecule/polymer memories, in which the inorganic nanomaterials or small molecules play the role of carriers capture sites.[17,43] Note that the device fabricated by pure PMMA without P3HT polymers showed no obviously electrical switching behavior.[42–44] Consequently, the conducting P3HT polymers in the PMMA matrix act as a crucial role for the bistable memory effect. After the device was switched to the high-current ON state, the current flow though the RSOM can be well modeled by the Ohmic law ($\alpha \sim 1$). This Ohmic current in the ON state is not affected by the space charges existed in the traps; accordingly, the high ON-state current may go through a local low-resistive conducting pathway such as metallic filament. Namely, the electrical switching might be attributed to the low-resistive conducting bridge formation in the polymer composite film connecting the bottom and top electrodes, leading the high current flow through the device. The high-current ON state can be retrieved to the initial low-current OFF state by applying a negative bias sweep with no current compliance, implying that the conducting metallic bridge can be ruptured by joule heat. As a result, the bipolar switching behaviors can be realized in our RSOM. In the presented RSOM, no metal component was used in the middle polymer film; therefore the metallic bridge might arise from the diffusion of the top Al electrode. Those Al particles might penetrate into the defective polymer matrix during the applying positive bias and the thermal evaporation of the Al electrode.[42,44,46]

To further confirm the conductivity switching behaviors of the rewritable RSOM, we then measured the impacts of PMMA concentrations (**Figure 5**a), the effect of film thickness of the polymer matrix (Figure 5b), and the area dependence experiments (Figure 5c). The effect of PMMA content in the polymer matrix for conductivity switching behaviors, including ON-current, OFF-current, and ON/OFF ratio, is summarized in Figure 5a. As shown in Figure 5a, the devices made from solution containing higher than 36 mg $mL^{-1}$ PMMA are of a quite low current level of $10^{-12}$–$10^{-11}$ A both in OFF- and ON-states with ON/OFF current ratio less than 5, which indicates that the electrical switching behavior of the RSOM is greatly hindered by a more strengthened PMMA matrix in the active layer (Figure S3 in Supporting Information). This PMMA concentration dependence of the electrical switching behavior is consistent with our proposed mechanism that as increasing the concentration of PMMA, the metal particles may be blocked by the reinforced PMMA matrix, which accordingly stops the bipolar conductivity switching effect. Furthermore, the effect of film thickness of the polymer matrix is summarized in Figure 5b. As shown in Figure 5b, the turn-on voltage is proportional to the thickness of polymer matrix (Figure S4 in Supporting Information), which results from a longer distance for metal particles migration. Another indirect evidence can be also obtained by the fact that the ON-state current level is insensitive to the top Al electrode area. As shown in Figure 5c, the ON-state of the devices reveals in a similar current level with respect to different electrode areas. This can be understood that the current flow arises from

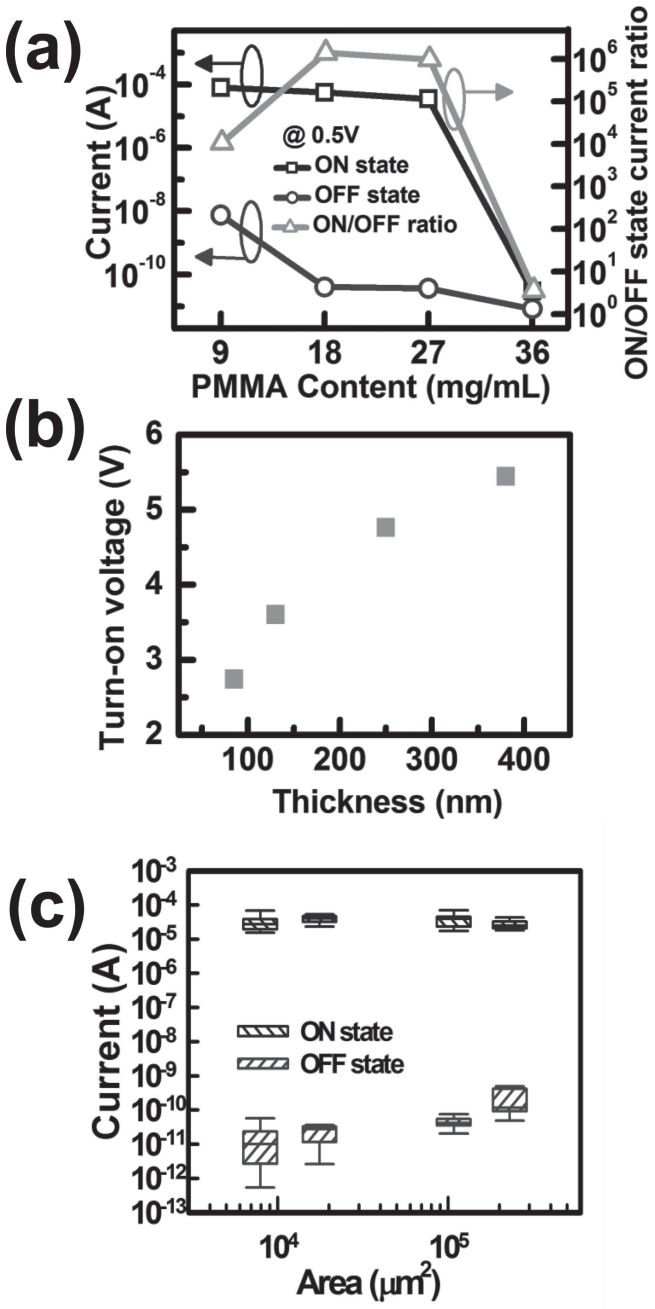


**Figure 5.** a) Effect of the PMMA content on the OFF-state, ON-state current, and ON/OFF state current ratio of the Al/PMMA:P3HT/graphene devices. b) Effect of the thickness of the polymer matrix on the turn-on voltage. c) Cell area dependence of the ON- and OFF- state current.

a localized high conductivity metallic path, which connects the top Al electrode to the bottom graphene film. Hence, the ON-state current flow weakly depends on the electrode area.[47]

Previous literature also reported the use of vertically phase-separated PMMA and P3HT to realize electrical bistable effect by trapping charge in the PMMA/P3HT interface.[48] However, in that case, the device needed further baking processes to induce perfect vertical phase separation, and the writing bias was negatively applied onto Al electrode with no current

compliance, which is different from the metal bridge phenomena occurred in our devices. Additionally, the retrievable electrical switching behavior of the RSOM is also quite different from our previously reported WORM-type memories fabricated by high ratio of conjugating polymer (P3BT) in the solution-type of PMMA insulator with co-solvent of anisole and CB.[35] The different results might be due to the fact that the percolation phenomenon caused by the higher density of conducting polymer was responsible for the un-retrievable electrical switching behaviors in our preliminary work.

Based on the above results as well as the analysis of the *I–V* curves, the erasable electrical switching effects can be understood as follows. The P3HT polymer with $\pi$-conjugation on its backbone can serve as the charge capture sites within the defective PMMA matrix. Initially, as applying a low positive bias on the Al electrode, the charge carriers emitted from the electrode would be injected into the PMMA polymer layer by Schottky emission. When the bias increased to ≈2.8 V, numerous of injected carriers from the electrode were captured in the P3HT trapping sites, resulting in the typical SCLC with a trap mode (known as TCLC). As the applied bias was increased, these captured charges created an intense local inner electric field in the PMMA matrix, and lured the Al particles penetrate into the polymer layer from the top toward bottom electrode. As a result, a conducting bridge is grown in the defective polymer layer under the intense inward field. Consequently, the memory device switched from a low-conductivity (OFF) state to a high-conductivity (ON) state. For the devices fabricated by pure PMMA polymer layer with no P3HT molecules presence, it cannot trap enough charges to generate sufficient internal electric field to form conducting filaments, leading to the fact that no obvious switching behavior was observed in the device.[42,44] And, notably, the current compliance applied from the forward sweep is to prevent the metal bridge over grown in the polymer layer. Consequently, the negatively sweeping with no current compliance can cause a higher joule heat to fracture the conducting bridge and recover the memory device to the low-conductivity (OFF) state.

It is worth giving a more detailed discussion on the difference of the underlying mechanisms between the newly presented re-writable SROM and our previous WORM-type one.[35] In our previous study, the dense commerical PMMA solution acts as a compact active layer to prevent the electrode metal particles from penetrating into the polymer film. Increasing the charge trapping media in the dense polymer matrix finally results in the percolation effect, which is responsible for the conductivity switching behavior in our previous memory devices. And, because the trapped charges cannot be extracted and neutralized, the previous memory devices therefore reveal a typical WORM-type memory. In order to develop a mass-practical moldable "re-writable" memory sticker, we elaborate a new conductivity switching scheme, that is, metal bridge formation, and formulate a suitable polymer compound. The defective insulating PMMA polymer formulated from PMMA powder plays one of the crucial roles in these electrical switching effect. The defective mezzanine with an intense inner electric field induced by a large number of trapped charges enables the metal particles to penetrate and form a conducting bridge in the polymer matrix, which realizes the conductivity switching effect in our newly-devised memory sticker. With a technological operation of current compliance, we can stop the metal bridge from overgrowing into the polymer matrix. Thus, after programming to the high conductivity state, a higher joul heat from a current compliance-free negative sweeping can rupture the conductive bridge and recover the memory devices to a low-conductivity state. Consequently, a more practical "re-writable" flash-type organic memory can be successfully designed in our new presented transferable and moldable organic memory sticker.

### 3.2. Discussion of the Sticker-Type Memory Film

Compared to traditional bottom-up solution processes for organic bistable memory, the transferable and re-writable sticker-type organic memory with an ultrathin ready-to-conduct flexible graphene electrode developed here might possess numerous unique advantages. Firstly, the exceptional transferable features of the organic memory pave an easy route to vertically integrate digital organic memories with other flexible organic devices with minimal solvent issue. This result may benefit to the development of future soft organic-based modules, including flexible and stretchable paper-like displayer, wearable computer or artificial smart skin. Secondly, the combination of organic memory and protective layer for transferring graphene electrode efficiently elided the chemical treatment processes to the protective layer. Accordingly, with the flexible and self-adhesive graphene-electrode underlay, the RSOM can be simply molded and functioned on other organic devices or arbitrary non-conventional substrates, including rough, non-planar, and soft ones. Thirdly, because both of the organic materials and the bottom CVD-graphene possess the capability for roll-to-roll processes, the resulting RSOM may suitable for industrial large-area printing production. Finally, the re-writable feature of a transferable organic memory is a brand-new breakthrough progress for various applications including stacked soft electronics and multilayer organic memories. Therefore, the firstly demonstrated transferable and flexible re-writable organic memory film with self-protective and self-adhesive features may broaden the wide-required digital memory in different applications.

## 4. Conclusion

In summary, a rewritable, transferable, and flexible sticker-type organic memory has been successfully demonstrated on arbitrary nonconventional substrates for the first time through a simple, low-temperature and cost-effective one-step methodology. The RSOM based on CVD-graphene electrode can be fabricated by blending polymer composite (PMMA:P3HT in CB) following mature solution processes and facilities. The blending polymer layer can serve as the memory active layer as well as the protective layer during the transferring processes. After etching the supporting metal, the RSOM can be easily labeled onto arbitrary non-conventional substrates, including rigid, rough and non-planar ones, and retain its original functions. The erasable electrical bipolar switching behavior of the

RSOM can be understood by the metal bridge grown in the polymer layer. The newly designed sticker-type memory with rewritable feature and advantages of versatile substrate selection can greatly broaden memory devices applications in various areas. In addition, our work can also pave an easy route for the integration of digital storage devices with diversified novel soft electronics, such as flexible and wearable electronic modules.

## 5. Experimental Section

*Device Fabrication*: A polymer blending solution was prepared by mixing poly (methyl methacrylate) (PMMA, 18 mg, $M_w$ = 950 k, Sigma Aldrich Co.) and poly (3-hexylthiophene) (P3HT, 2 mg, $M_w$ = 40 k, Luminescence Technology Co.) in chlorobenzene (CB, 1 mL) with stirring at 50 °C for one day. Afterward, the as-prepared solution was spin-coated onto the graphene-grown copper foil at a rate of 2000 rpm for 20 s (≈130 nm by alpha step) followed by drying under reduced pressure. Subsequently, the underlay copper foil was dissolved by a Cu etchant, an aqueous solution of iron nitrate ($Fe(NO_3)_3$) (0.05 g $mL^{-1}$). Next, the sticker-type organic memory was firstly transferred to deionized water for washing away the Cu etchant, and then transferred onto the polyethylene terephthalate (PET) substrate or other target substrates and dried naturally. The top electrodes of the device, 300-nm-thick aluminum, were thermally deposited onto the top of sticker-type organic memory at a pressure of $2 \times 10^{-6}$ Torr through a shadow mask with circular patterns. The area of memory cell defined by the sandwich of the top Al electrode and graphene sheet was 0.23 $mm^2$.

*Measurement*: All of the electrical characterizations of the fabricated memory device were measured by a Keithley 4200 semiconductor parameter analyzer. All electrical properties were characterized at room temperature and ambient conditions.

## Supporting Information

Supporting Information is available from the Wiley Online Library or from the author.

## Acknowledgements

Y.C.L. would like to thank Chun-Yu Chang for his assistance in AFM experiment and also appreciate the scholarship from the Taiwan National Science Council (project no.102–2917-i-002–087). This work was supported by grants from National Science Council and Ministry of Education of the Republic of China.

Received: July 3, 2013
Revised: August 28, 2013
Published online: October 18, 2013

[1] D. H. Kim, N. Lu, R. Ma, Y. S. Kim, R. H. Kim, S. Wang, J. Wu, S. M. Won, H. Tao, A. Islam, *Science*, **2011**, *333*, 838–843.
[2] J. U. Park, S. Nam, M. S. Lee, C. M. Lieber, *Nat. Mater.* **2011**, *11*, 120–125.
[3] S. H. Kim, J. Yoon, S. O. Yun, Y. Hwang, H. S. Jang, H. C. Ko, *Adv. Funct. Mater.* **2013**, *23*, 1375–1382.
[4] Q. N. Thanh, H. Jeong, J. Kim, J. Kevek, Y. Ahn, S. Lee, E. D. Minot, J. Y. Park, *Adv. Mater.* **2012**, *24*, 4499–4504.
[5] C. H. Lee, D. R. Kim, X. Zheng, *Nano Lett.* **2011**, *11*, 3435–3439.
[6] K. Chung, C. H. Lee, G. C. Yi, *Science* **2010**, *330*, 655–657.
[7] C. H. Lee, D. R. Kim, I. S. Cho, N. William, Q. Wang, X. Zheng, *Sci. Rep.* **2012**, *2*, 1000.
[8] S. H. Chae, W. J. Yu, J. J. Bae, D. L. Duong, D. Perello, H. Y. Jeong, Q. H. Ta, T. H. Ly, Q. A. Vu, M. Yun, *Nat. Mater.* **2013**, *12*, 403–409.
[9] M. S. Mannoor, H. Tao, J. D. Clayton, A. Sengupta, D. L. Kaplan, R. R. Naik, N. Verma, F. G. Omenetto, M. C. McAlpine, *Nat. Commun.* **2012**, *3*, 763.
[10] A. K. Sharma, *Advanced Semiconductor Memories: Architectures, Designs, and Applications* Wiley-IEEE Press, Piscataway, NJ, **2003**.
[11] J. J. Yang, D. B. Strukov, D. R. Stewart, *Nat. Nanotechnol.* **2012**, *8*, 13–24.
[12] R. Waser, M. Aono, *Nat. Mater.* **2007**, *6*, 833–840.
[13] T. C. Chang, F. Y. Jian, S. C. Chen, Y. T. Tsai, *Mater. Today* **2011**, *14*, 608–615.
[14] J. Ouyang, C. W. Chu, C. R. Szmanda, L. Ma, Y. Yang, *Nat. Mater.* **2004**, *3*, 918–922.
[15] R. J. Tseng, C. Tsai, L. Ma, J. Ouyang, C. S. Ozkan, Y. Yang, *Nat. Nanotechnol.* **2006**, *1*, 72–77.
[16] B. Cho, S. Song, Y. Ji, T. W. Kim, T. Lee, *Adv. Funct. Mater.* **2011**, *21*, 2806–2829.
[17] Y. Ji, S. Lee, B. Cho, S. Song, T. Lee, *ACS Nano* **2011**, *5*, 5995–6000.
[18] Q. D. Ling, D. J. Liaw, C. Zhu, D. S. H. Chan, E. T. Kang, K. G. Neoh, *Prog. Polym. Sci.* **2008**, *33*, 917–978.
[19] A. Hadipour, B. de Boer, J. Wildeman, F. B. Kooistra, J. C. Hummelen, M. G. Turbiez, M. M. Wienk, R. A. Janssen, P. W. Blom, *Adv. Funct. Mater.* **2006**, *16*, 1897–1903.
[20] T. W. Kim, D. F. Zeigler, O. Acton, H. L. Yip, H. Ma, A. K. Y. Jen, *Adv. Mater.* **2012**, *24*, 828–833.
[21] A. K. Geim, K. S. Novoselov, *Nat. Mater.* **2007**, *6*, 183–191.
[22] K. S. Kim, Y. Zhao, H. Jang, S. Y. Lee, J. M. Kim, K. S. Kim, J. H. Ahn, P. Kim, J. Y. Choi, B. H. Hong, *Nature* **2009**, *457*, 706–710.
[23] Y. Lee, S. Bae, H. Jang, S. Jang, S. E. Zhu, S. H. Sim, Y. I. Song, B. H. Hong, J. H. Ahn, *Nano Lett.* **2010**, *10*, 490–493.
[24] O. Frank, G. Tsoukleri, J. Parthenios, K. Papagelis, I. Riaz, R. Jalil, K. S. Novoselov, C. Galiotis, *ACS Nano* **2010**, *4*, 3131–3138.
[25] G. Tsoukleri, J. Parthenios, K. Papagelis, R. Jalil, A. C. Ferrari, A. K. Geim, K. S. Novoselov, C. Galiotis, *Small* **2009**, *5*, 2397–2402.
[26] G. Eda, G. Fanchini, M. Chhowalla, *Nat. Nanotechnol.* **2008**, *3*, 270–274.
[27] X. Huang, Z. Zeng, Z. Fan, J. Liu, H. Zhang, *Adv. Mater.* **2012**, *24*, 5979–6004.
[28] Q. He, S. Wu, Z. Yin, H. Zhang, *Chem. Sci.* **2012**, *3*, 1764–1773.
[29] A. Reina, X. Jia, J. Ho, D. Nezich, H. Son, V. Bulovic, M. S. Dresselhaus, J. Kong, *Nano Lett.* **2008**, *9*, 30–35.
[30] A. Reina, H. Son, L. Jiao, B. Fan, M. S. Dresselhaus, Z. Liu, J. Kong, *J. Phys. Chem. C* **2008**, *112*, 17741–17744.
[31] S. P. Koenig, N. G. Boddeti, M. L. Dunn, J. S. Bunch, *Nat. Nanotechnol.* **2011**, *6*, 543–546.
[32] S. Lee, G. Jo, S. J. Kang, G. Wang, M. Choe, W. Park, D. Y. Kim, Y. H. Kahng, T. Lee, *Adv. Mater.* **2011**, *23*, 100–105.
[33] J. Liu, Z. Yin, X. Cao, F. Zhao, A. Lin, L. Xie, Q. Fan, F. Boey, H. Zhang, W. Huang, *ACS Nano* **2010**, *4*, 3987–3992.
[34] J. Liu, Z. Zeng, X. Cao, G. Lu, L.-H. Wang, Q.-L. Fan, W. Huang, H. Zhang, *Small* **2012**, *8*, 3517–3522.
[35] Y. C. Lai, F. C. Hsu, J. Y. Chen, J. H. He, T. C. Chang, Y. P. Hsieh, T. Y. Lin, Y. J. Yang, Y. F. Chen, *Adv. Mater.* **2013**, *25*, 2733–2739.
[36] S. Bae, H. Kim, Y. Lee, X. Xu, J. S. Park, Y. Zheng, J. Balakrishnan, T. Lei, H. R. Kim, Y. I. Song, *Nat. Nanotechnol.* **2010**, *5*, 574–578.
[37] X. Li, W. Cai, J. An, S. Kim, J. Nah, D. Yang, R. Piner, A. Velamakanni, I. Jung, E. Tutuc, *Science* **2009**, *324*, 1312–1314.

[38] Z. Wang, F. Zeng, J. Yang, C. Chen, F. Pan, *ACS Appl. Mater. Interfaces* **2011**, *4*, 447–453.
[39] S. M. Sze, *Physics of Semiconductor Devices* Wiley, New York **1981**.
[40] K. C. Kao, W. Hwang, Electrical Transport in Solids, B. R. Pamplin, Ed., *International Series in the Science of Soild State* Pergamon, New York **1981**.
[41] P. Kumar, A. Misra, M. Kamalasanan, S. Jain, V. Kumar, *J. Phys. D Appl. Phys.* **2007**, *40*, 561.
[42] D. I. Son, T. W. Kim, J. H. Shim, J. H. Jung, D. U. Lee, J. M. Lee, W. I. Park, W. K. Choi, *Nano Lett.* **2010**, *10*, 2441–2447.
[43] D. I. Son, D. H. Park, W. K. Choi, S. H. Cho, W. T. Kim, T. W. Kim, *Nanotechnology* **2009**, *20*, 195203.
[44] D. I. Son, J. H. Shim, D. H. Park, J. H. Jung, J. M. Lee, W. I. Park, T. W. Kim, W. K. Choi, *Nanotechnology* **2011**, *22*, 295203.
[45] Z. Chiguvare, V. Dyakonov, *Phys. Rev. B* **2004**, *70*, 235207.
[46] D. Tondelier, K. Lmimouni, D. Vuillaume, C. Fery, G. Haas, *Appl. Phys. Lett.* **2004**, *85*, 5763.
[47] T.-W. Kim, H. Choi, S.-H. Oh, M. Jo, G. Wang, B. Cho, D.-Y. Kim, H. Hwang, T. Lee, *Nanotechnology* **2009**, *20*, 025201.
[48] W. S. Song, H. Y. Yang, C. H. Yoo, D. Y. Yun, T. W. Kim, *Org. Electron.* **2012**, *13*, 2485–2488.